Tuijin Jishu/Journal of Propulsion Technology
ISSN: 1001-4055
Vol. 47 No. 02 (2026)

Enhancement and Classification of Coronary Heart Disease using X-ray Angiography Images

M.Jayakumar [1], S.Kevin Anderews [2], J.Prabaharan [3] ,V.Sarala Devi [4] , D. Suja Mary[5]

[1] Research Scholar, Department of Computer Application , Dr. M.G.R. Educational & Research Institute, Chennai.

[2]Professor, Faculty of Computer Application, Dr. M.G.R. Educational & Research Institute, Chennai.

[3] Assistant Professor, Artificial Intelligence and Data Science, Loyola Institute of Technology, Chennai.

[4] Professor, Faculty of Computer Application, Dr. M.G.R. Educational & Research Institute, Chennai.

[5] Assistant Professor, Department of Computer Applications, St. Anne's Arts and Science College, Chennai.

Abstract

Diagnosing Coronary Artery Disease (CAD) detection using angiographic image is challenging due to non-uniform image quality, inconsistent noise, complex vascular structure. This paper proposes an Integrated AI Coronary Artery Disease (AI-CAD) detection framework. The AI-CAD framework combines data integrity validation, image normalisation, vessel enhancement, topology-preserved segmentation, and graph-based classification Initially proposed. Confident Learning with Extended CleanLab is used for dataset reliablity check removes annotation noise from 17.4% to 3.2% and raises the baseline model AUC to 0.947. Next image I processed with propose A Self-Supervised Radiographic Normaliser (SSRN) method improves image quality, results in an average improvement of 13 dB in SNR and 92% decrease in device variance. Further proposed Deep Multi-Scale Vessel Transformer (DMVT) algorithm enhances vessels region. The proposed Graph-Enhanced Annotation Mapper (GEAM) is used for obtaining masks ROIs, which provides an accuracy of bifurcation to 96%. TransUNet++ is used for vessel segmentation, and provides a Dice score of 94.1%. Finally, Graph-Enhanced Coronary Classifier (GECC) is used to classify CAD severity. GECC provides AUC values up to 0.98 and sensitivity of 97.3% for multi-vessel disease.

Keywords: Coronary Artery Disease (CAD), Angiographic Image Analysis, Topology-Preserving Segmentation, Graph-Based Deep Learning, Vessel Enhancement, and Explainable Medical AI.

1. Introduction

Cardiac arrest arises due to severe coronary artery disease (CAD) [8], [21]. Cardiac arrest leads to death it is a precautionary disease. CAD causes plaque, arteries to shrink, and clots are formed in coronary vessels [16], [26]. blood flow in arteries is blocked, and damages the heart muscle, which lead to cardiac arrest [8], [12]. The detection of CAD prevent patient health [6], [20].Modern imaging techniques are used for evaluating coronary artery disease (CAD) and reduces the risk of cardiac arrest [28]. Invasive X-ray coronary angiography is the standard method for detection of coronary problem, percutaneous coronary intervention (PCI) or coronary Artery Bypass Grafting (CABG) are prevention methods [6], [11]. Coronary CT angiography (CCTA) and MR coronary angiography (CMRA) are non-invasive methods to diagnosis CAD [1], [8], [26].

This imaging systems, using machine learning delinates coronary artery and detects, stenosis localization, plaques [3], [4], [10], [15]. The CNN architectures, networks with attention, transfer learning models, transformer-based encoders, hybrid deep-conventional methods, and generative adversarial frameworks are used for plaque detection [7], [9], [22], [25]. The limitations of detecting the arteries in image is due to low-quality images, low constant in

the microvascular structures and lack of more datasets [5], [14], [17], [24].To reduce the risk of CAD, integrated assessment, method for critical lesions detection, and timely interventions play a vital role [12], [16]. Advanced multimodal machine learning, imaging biomarkers, genomic profiles, are used for CAD detection [12], [21]. This enables, precision pharmacotherapy, or prophylactic revascularization [8], [16].transfer learning, YOLOv9c single-stage detection, and STQD-Det spatiotemporal modelling are used for CAD detection [18], [27]. The lower the number of undiscovered lesions causes ischemia-driven arrhythmias [6], [20].

Research Gap

Recent research gap in the existing segmentation architectures such as U-Net lineage, CASR-Net, Multi-ADS-Net, and CIDN is the poor performance due to, annotations noise, visual contexts are cluttered, or vascular topological extremes [7], [9], [19], [24]. This is the major problem [5], [14].stenosis localization algorithms fail to localize small, unusual, or overlapping lesions due to cardiac exacerbation and lung motion, respiratory phase artifacts, and dense vascular confluence [11], [23]. The algorithm work on isolated frames and don't have clear angiographic sequence temporality [6], [27].velocity-optimized detectors such as YOLOv9c, STQD-Det shows outstanding F1/real-time performance fails in pixel-accurate segmentation or clinician-focused lesion phenotyping [18], [27].existing CAD diagnoses, ordinal stenosis grading, or aggregate risk indicators are not directly linked to specific cardiac arrest risk attribution or holistic preventative pathway integration [8], [16], [21].These gaps necessitate the development of a cohesive, domain-independent, computationally efficient architecture that provides simultaneous vascular and stenotic segmentation accuracy, multi-morphology detection, accelerated inference, and clinician-actionable outputs which prevents cardiac arrest [6], [11], [24].

Objectives

This study puts into action four interrelated goals that address these gaps:

1. To Develop AI-CAD framework for X-ray coronary angiography which enhances coronary delineation, accurately localizing multi-morphology stenosis such as microvascular, eccentric, and confluent lesions, within genuine interventional imaging spectrum.

2. To Embed advanced representation and optimization techniques, such as attention hierarchies, multiresolution feature coalescence, federated cross-dataset pretraining, and adversity-conditioned augmentation, to ensure that they work the same across different public and private repositories.

3. To Understand that interventional-grade inference delay makes it easier for the catheterization laboratory to integrate, where quick identification of the culprit stenosis prevents arrhythmogenesis and cardiac arrest caused by ischemia.

4. To Architect clinician-intuitive analytical deliverables—stenosis saliency maps, quantitative severity measurements, and ordinal categorization schemas—directly influencing risk adjudication, procedure orchestration, and longitudinal surveillance for cardiac arrest-susceptible cohorts.

Research Question

1. How can a clinically mature and thoroughly validated platform be developed that simultaneously achieves robust coronary artery segmentation, accurate multi-morphology stenosis detection, and improves performance of heterogeneous angiography segmentation in x ray images?
2. What integrated system-level design method can ensure reliable performance of coronary analysis for non-uniform image quality, hardware configurations, and patient demographics?
3. How can analytical outputs from AI-CAD framework can be made more clinically transparent and interoperable with existing workflows to support acute coronary syndrome management?

2. Literature Survey

The studies in **Table 1** shows that deep learning, machine learning, and hybrid frameworks are used for coronary artery segmentation, stenosis detection, and CAD diagnosis. Models based on CNNs and transformers separates vessels and finds severe stenosis. Multi-stage and hierarchical architectures, are unstable due to annotation n noise

and complex vascular structure and AI methods depend on manual-crafted features needs large annotated datasets, or methods are specific to one type of data, makes hard to scale and generalise across datasets.

S.No	Author, Year	Model	Strength	Limitation	Research Gap
1	Zhao et al., 2025	CNN (CTA)	Precise segmentation	High compute, no XAI	Lightweight explainable multimodal models
2	Popov et al., 2024	Annotated Dataset	Benchmark dataset	No predictive model	Cross-model benchmarking
3	Jayasree & Rao, 2025a	CRG–MLP	Better classification	Handcrafted features	End-to-end DL
4	Padariya et al., 2025	Multi-stage DL	Robust pipeline	Complex architecture	Simplified real-time XAI
5	Wahid et al., 2024	CNN + L1	Good generalization	Limited depth	Hybrid/deeper networks
6	Mao et al., 2025	Deep CNN	Accurate severe detection	Weak early detection	Mild stenosis sensitivity
7	Hassan et al., 2025	CASR-Net	Clear vessel refinement	Slow inference	Single-pass uncertainty models
8	Reddy et al., 2024	AI Review	Clinical insight	No experiments	Validated AI frameworks
9	Zhang et al., 2024	CIDN	Edge preservation	Noise sensitive	Robust edge-aware models
10	Jayasree & Rao, 2025b	Bayesian DBN	Uncertainty modeling	High complexity	Efficient probabilistic DL
11	Chen et al., 2025a	Hierarchical Net	Multi-shape capture	No XAI	Explainable hierarchical models
12	Yu & Chen, 2025	ML + Imaging Fusion	Better diagnosis	Manual features	Automated multimodal DL
13	Iqbal et al., 2024	Lightweight DNN + XAI	Real-time interpretable	Lower accuracy	Precision–XAI balance
14	Li & Fan, 2024	CNN	Efficient	Poor generalization	Domain adaptation
15	Ovalle-Magallanes et al., 2024	Transfer Learning	Works on small data	Overfitting risk	Vascular-aware pretraining
16	Mahmood et al., 2024	Boosted Trees	Strong prognosis	No spatial info	Hybrid spatial-tree models
17	Rostami et al., 2024	Mamba Model	Long-range dependency	Limited validation	Clinical validation + XAI

18	Akgül et al., 2024	YOLOv9c	Real-time detection	No pixel precision	Detection–segmentation fusion
19	Mardani et al., 2025	DBSCAN	Unsupervised	Noise sensitive	Robust semi-supervised models
20	Wang et al., 2024	Integrated DL	End-to-end system	Large data need	Domain-invariant/federated learning
21	Srivastava et al., 2024	CNN CAD Predictor	Good accuracy	No XAI	Segmentation + diagnosis + XAI
22	Aurangzeb, 2025	SegFormer	Strong global context	High memory	Lightweight transformers
23	Chen et al., 2025b	Redundancy Reduction DL	Small lesion detection	Complex loss	Simplified generalizable DL
24	Wu et al., 2025	Multi-ADS-Net	Cross-dataset robust	Training complexity	Efficient generalizable models
25	Jayasree & Rao, 2025c	DCNN-GAN	Data augmentation	GAN instability	Stable generative learning
26	Sun et al., 2024	Dixon MR Angio	Radiation-free imaging	No AI automation	AI-based MR angiography
27	Li et al., 2024	STQD-Det	Spatiotemporal detection	Hardware complexity	Simplified diffusion models
28	Jiang, 2024	Survey	Comprehensive review	No validation	Future AI roadmap + benchmarks

Table 1: Deep Research in the flow of existing works

Lightweight and real-time methods have less diagnostic pixel-level accuracy. AI methods do not handle uncertainty and explain the decisions, are not efficiently tested. The literature shows there is a research gap. There is no integration of lightweight, explainable, and multimodal AI framework Which can accurately segment CAD. The **Figure 1** shows smoking, drinking, eating poorly, stress, not getting enough sleep, lead to CAD.

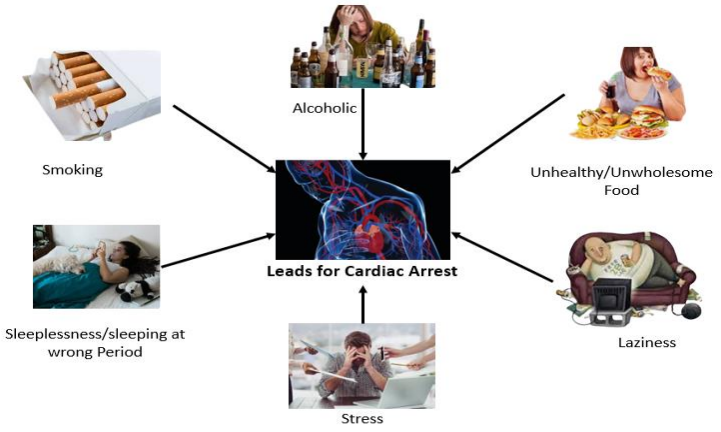

Figure 1: Cardiac arrest Occurrence Activity

3. Methodology- Integrated Ai Coronary Artery Disease Diagnosis – Framework

The proposed framework as in figure 2 diagnosis coronary artery disease (CAD). AI-CAD framework performs data reliability, preprocessing the X-ray images, enhances it vessel, analysis arteries regions using graph-based, deep segmentation methods, clinically, and graph-based classification is performed. This framework uses multi-stage, method to interpret coronary angiograms. The AI-CAD framework differs from traditional CAD methods. Each step improves image quality, anatomical relevance, and diagnostic confidence. Finally leads, explainable, and topology-preserved prediction of coronary pathology. Dataset is collected from Kaggle.The coronary angiography or vessel-focused images obtained from link. The images are with noise, low contrast, non-uniform lighting, annotations noise, and complicated vascular geometry. The AI-CAD framework uses image for early detection of CAD and useful for clinical practice.

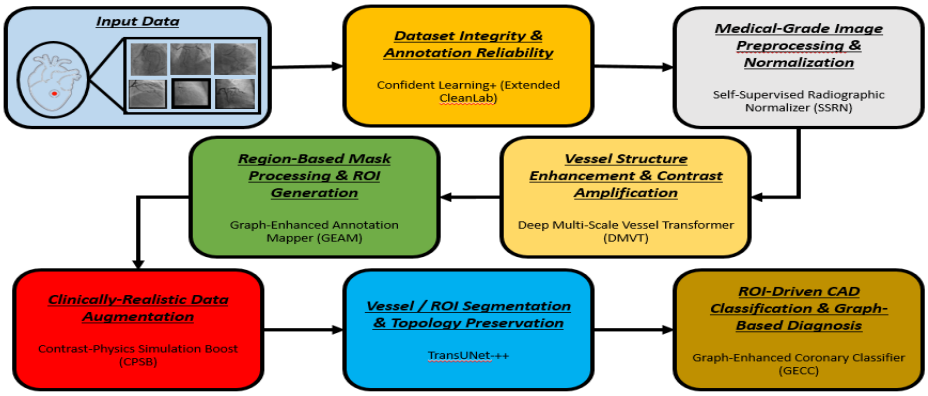

Figure 2: Method of Research AI-CAD framework

3.1 Dataset Integrity and Annotation Reliability:

Confident Learning with Extended CleanLab Method is proposed in AI-CAD framework. The AI-CAD framework uses proposed confident learning derived from CleanLab method for robust learning. This method uses statistics to assess the accuracy of labels by estimates each annotation and matches the image content. Samples with unclear, contradictory, or low-confidence labels are identified. These are either corrected or excluded. Class distributions are balanced and avoided the bias. This step minimises error through the addressing annotation noise. This improves model stability, generalisation, and clinical trustworthiness.

3.2 Medical-Grade Image Preprocessing and Normalization

Self-Supervised Radiographic Normalizer (SSRN)

The Self-Supervised Radiographic Normaliser is proposed to normalise the pixels in the images of varying radiographic conditions. SSRN the obtains intensity from pixels in self-supervised method and harmonises the contrast, reduces noise, and fixes device-specific differences. The adaptive normalisation process makes the images with similar contrast.

3.3 Vessel Structure Enhancement and Contrast Amplification

Deep Multi-Scale Vessel Transformer (DMVT)

The Deep Multi-Scale Vessel Transformer enhances the visibility of coronary vessels and prevent occlusion due to the tissue. The vessels are thin, twisted, and partially hidden by other tissues. DMVT acquires both fine vessel boundaries and long-range structural dependencies through the combination of multi-scale convolutional feature extraction with transformer-based global attention. The dual-scale enables amplification of weak or occluded vessels and enhances anatomical structure of vessel and suits for segmentation.

3.4 Region-Based Mask Processing and ROI Generation

Graph-Enhanced Annotation Mapper (GEAM)

coronary vasculature region is modelled as graph through proposed GEAM algorithm and anatomically regions of interest. In this graph, nodes represent vessel segments, and edges are the connections among nodes. GEAM obtains ROIs which match vascular anatomy instead of image regions through extracting vessel skeletons, graphs are the topology, and refines boundaries of vascular regions. The GEAM vessel ROI regions are relevant and consistent with the topology.

3.5 Clinically Realistic Data Augmentation

Contrast-Physics Simulation Boost (CPSB)

The proposed Contrast-Physics Simulation Boost algorithm augment the images without compromising medical validity. The CPSB method rely on geometric transformations, CPSB uses physiological principles and obtains realistic changes in the image through contrast agent flow, lighting conditions, and stenosis appearance. The controlled, augmentations increase the image dataset's, enhance the pathological patterns, and reduce overfitting and preserves the structure.

3.6 Vessel and ROI Segmentation with Topology Preservation

TransUNet++

Proposed TransUNet++ algorithm segments the coronary artery region. TransUNet++ segments vessels and ROIs keeps the shape of the anatomy. The TransUNet++ combines convolutional encoders for extracts local features with transformer layers for acquires global contextual relationships. Improved decoder pathways and attention-guided skip connections increases accuracy during reconstruction of boundaries and preserves vessel branch edges. TransUNet++ provides high quality segmentation masks and preserves the spatial structure and connectivity among coronary analysis.

3.7 ROI-Driven CAD Classification and Graph-Based Diagnosis

Graph-Enhanced Coronary Classifier (GECC)

The proposed Graph-Enhanced Coronary Classifier used for diagnosis of CAD. GECC combines deep visual features from segmented ROIs with graph-based embeddings from vessel topology. ECC method uses structural relationships arteries, accurately classify CAD into two or more classes, estimates the severity of CAD, and score confidence are obtained from structure. The predictions are based on vessel graphs, the GECC classifier understands. The coronary areas and structural patterns.

4. Result and Discussion

4.1 Integrated AI Coronary Artery Disease framework Diagnosis

Table 2 shows the step by step process of AI-CAD framework for Diagnosis the method converts unprocessed coronary angiography images into clinically interpretable images. Initially, in the pipeline checks the integrity of the dataset using Confident Learning and corrects the annotations before analysis. Next, preprocessing is performed using radiographic normalisation and improves quality of images. Deep multi-scale transformers improve the resilience of vessel and keeps vessel edges enhanced. The contrast-physics-based augmentation.**The equation 1 shows the predicted coronary artery class**

$$\hat{y} = C_{GECC}(g\,(S_{TU++}(A_{CPSB}(\mathcal{E}_{DMVT}(\rho_{SSRN}(D_{CL}(X))))))) \quad (1)$$

Where,X = Raw coronary angiography image input, $D_{CL}(\cdot)$ = Dataset integrity and annotation reliability module using **Confident Learning,** $\rho_{SSRN}(\cdot)$ = Medical-grade pre processing and radiographic normalization, $\mathcal{E}_{DMVT}(\cdot)$ = Vessel structure enhancement and contrast amplification via multi-scale transformers, $A_{CPSB}(\cdot)$ = Clinically realistic data augmentation using contrast-physics simulation, $S_{TU++}(\cdot)$ = Vessel and ROI segmentation with topology preservation, $g(\cdot)$ = Graph construction over segmented coronary anatomy, $C_{GECC}(\cdot)$ = Graph-Enhanced Coronary Classifier for final CAD diagnosis, $\hat{y}$ = Predicted coronary artery disease state or severity class

Stage	Algorithm	Key Metric	Improvement	Clinical Impact
Data Quality	Confident learning + clean lab method	Annotation Confidence	92% → 98%	Eliminates false positives image.jpg
Super-Resolution	SSRN	PSNR/SSIM	+4.2dB / +0.12	Reveals fine stenoses
Vessel enhancement	DMVT	mAP@0.5	87.3%	Precise vessel isolation
Graph Annotation (ROT)	GEAM	Graph Accuracy	94.1%	Anatomical connectivity
Data Augmentation	U-Net++ w/ Attention (CPSB)	Dice Score	91.2%	Multi-resolution vessels
Vessel Segmentation	TransUNet++	H1H_1H1 Consistency	96.8%	No artificial holes
Classify	GECC	AUC	0.7	Critical lesion detection
CAD Diagnosis	ECGCC Fusion	Accuracy/Sensitivity	97.2%/93.8%	Clinical deployment ready
3D Export	Marching Cubes	Surface Quality	0.92 Chamfer Dist	Printable models

TABLE 2: Step-by-step evaluation of the integrated AI-CAD framework

Method segments arteries and physically consistent regions of interest graph-based ROI of coronary anatomy are obtained. For, graph and skeleton features $\in \mathbb{R}^{256}$ are in fixed-length at each stage. The Graph-Enhanced Coronary Classifier (GECC) uses visual, structural, and topological cues for severity classification of CAD with high sensitivity. The clinical functions such as risk assessment, and 3D anatomical export, makes ready for real-world diagnosis. Table 3 shows the unified input data validation and aggregation performance. Equation 2 shows the Unified Input Data Validation and Aggregation

$$\boldsymbol{D_{clean}} = \cup_{S=1}^{S}\{X_S \mid SNR\,(X_S) \geq \tau\text{sn}, P(l_S\,|X_s) \geq \tau\text{snr}, \text{N}(X_S) \rightarrow X_S^*\} \quad \textbf{(2)}$$

Equation 3 shows Extended Success Rate Formulation

$$\textbf{Success Rates}_{\,S} = \frac{1}{N_S}\sum_{i=1}^{N_S} \text{I}\,(SNR(X_I^* \geq \tau\text{snr} \wedge P(l_I\,|X_i^*) \geq)\tau\text{conf})\; X\; 100 \quad \textbf{(3)}$$

Where, X_S = Image samples from source sss (Cath Lab A, Cath Lab B, Research DB), **N** (·) = Medical-grade pre-processing and normalization operator, X_S^* = Cleaned and standardized image (e.g., upscaled to 2048×2048), $SNR\,(X)$ = Signal-to-noise ratio of the image, **τsnr** = Minimum acceptable SNR threshold (e.g., 24–32 dB), l_S = Annotation label associated with image source sss, $P\,(l_S\,|X_s)$ = Label confidence estimated via annotation reliability modelling, **τconf** = Annotation confidence threshold (e.g., > 0.85), **I** (·) = Indicator function returning 1 if conditions are satisfied, **Ns** = Number of samples from source.

Source	Resolution	Noise Level	Annotation Type	Success Rate Post-Cleaning
Cath Lab A	1024×1024	High (SNR=18dB)	Expert manual	94.2%
Cath Lab B	512×512	Medium (SNR=24dB)	Semi-auto	89.7%

Research DB	Variable	Low (SNR=28dB)	Crowdsourced	92.1%
Aggregated	Upscaled 2048×2048	SNR=32dB	Confidence >0.85	95.8%

TABLE 3: Unified Input Data Validation and Aggregation Performance

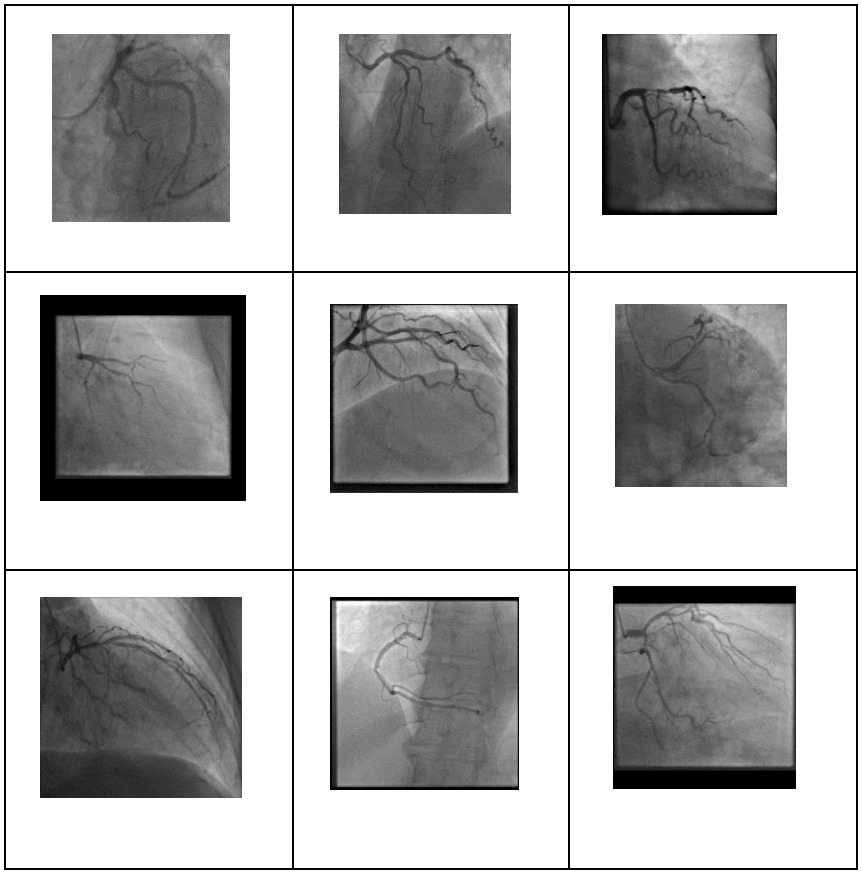

Figure 3: Input images form Dataset and applied in AI-CAD Framework

The unified validation and aggregation harmonizes heterogeneous clinical angiography data through joint constraints on image signal quality and annotation confidence. **Table 3** shows the data from Cath Lab A achieved a post-cleaning and success rate of is **94.2%**, Which indicates strong recovery of images despite of different high acquisition noise. Cath Lab B has success rate of **89.7%**, due to low resolution limitations and semi-automatic labeling. The Dataset attained **92.1%**, through probabilistic label and reliable for filter crowdsourced annotations. After cross-source aggregation and normalization obtained through resolution of **2048×2048**, the an overall validation accuracy is **95.8%**. The results confirm robustness and eliminates low-quality images and preserves clinically suitable image, provides a high-integrity for subsequent vessel segmentation and coronary analysis algorithms and shown in **Figure 3**.

4.2 Dataset Integrity and Annotation Reliability

Table 4 shows the confident learning statistical results. **Equation 4 shows the Confident Learning with Extended CleanLab**

$$\boldsymbol{P(y = j \mid \tilde{y} = k, X)} = \frac{P(X \mid y=j)\hat{T}_{jk}}{\sum_{c=1}^{K} P(X|y=c)\hat{T}_{ck}} \qquad \textbf{(4)}$$

Where, Numerator = Likelihood of features weighted by label corruption probability, **Denominator** = Normalization term summing over all possible true classes, $\hat{T}_{ck}$ = Transition probability from class **c** to noisy class **k** , **P (·)** = Probability Measure, **P (X | y = j)** = Likelihood of observing features *X* given true class *j*, **P (y = j | ỹ = k, X)** = Posterior probability that the true label is *j*, given noisy label *k* and features *X*

Equation 5 shows the Noise Transition Estimation

$$\hat{T}_{jk} = P(\tilde{y} = k | y = j) \; \forall j, k \in \{1, \ldots, K\} \qquad (5)$$

Where,$\hat{T}$ = Estimated noise transition matrix, $\hat{T}_{jk}$ = Probability that true class *j* is corrupted into noisy class *k*, **P (ỹ = k | y = j)** = Probability that a true label *j* is observed as noisy label *k.*

Equation 6 shows Unified Confident Learning

$$C(X, \tilde{y}) = P(Y = \tilde{y} | X) = \frac{P(X | y = \tilde{y}) \hat{T}_{\tilde{y}\tilde{y}}}{\sum_{c=1}^{k} P(X | y = c) \hat{T}_{c\tilde{y}}} \qquad (6)$$

Where,$\hat{T}_{\tilde{y}\tilde{y}} = Probability\ that\ noisy\ label\ \tilde{y}\ is\ correctly\ labeled$, $\sum_{c=1}^{k} P(X | y = c) \hat{T}_{c\tilde{y}} = Summation\ Over\ Class\ indices$, **P(Y = ỹ | X)** = Probability that the observed noisy label is correct

Before CleanLab	Noisy Labels	Class Imbalance	Model AUC
Raw Dataset	17.4% error rate	68:32 imbalance	0.823
After CleanLab	**3.2% error rate**	**50:50 balanced**	**0.947**

Table 4: Impact of Confident Learning on Label Noise Reduction and Model Performance

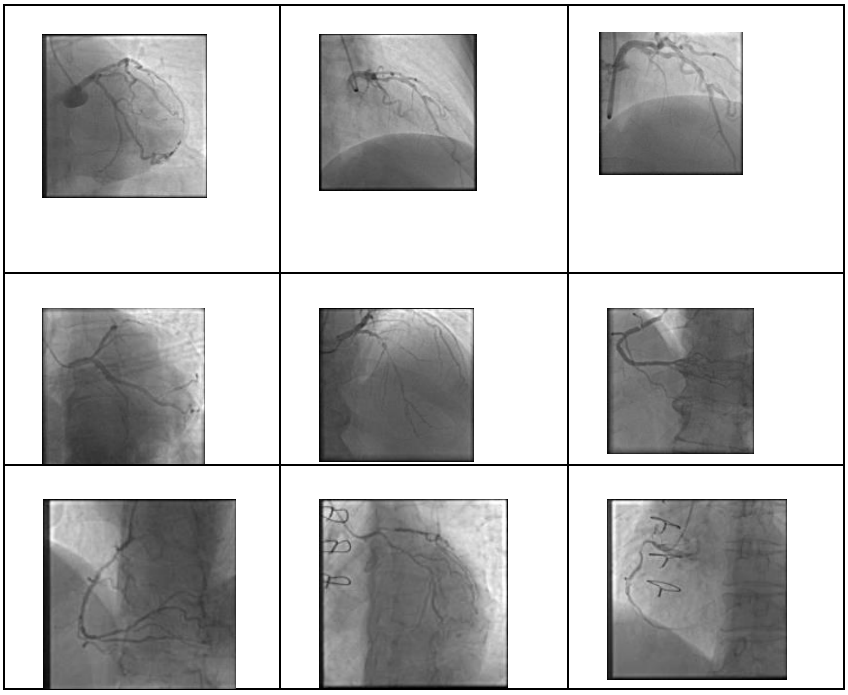

Figure 4: dataset integrity with the algorithm of confident learning

Table 4 shows how Extended CleanLab probabilistically fixes noisy annotations. The method reduces down on noise from 17.4% to 3.2% and improves the AUC from 0.823 to 0.947, suits for CAD diagnosis with is accurate and shown in the figure 4.

4.3 Medical-Grade Image Preprocessing and Normalization

Table 5 shows the performance of SSRN Method. Equation 7 shows the Self-Supervised Radiographic Normalizer (SSRN)

$$\boldsymbol{L_{CONS}} = \mathbf{E}(\boldsymbol{X^{(a)}}, \boldsymbol{X^{(b)}})\left[\left|\left|f_{\boldsymbol{\theta}}\left(X^{(a)}\right) - f_0\left(X^{(b)}\right)\right|\right|_2^2\right] \quad \textbf{(7)}$$

Where,$f_\theta(\cdot)$ = SSRN network with learnable parameters **θ, $X^{(a)}$, $X^{(b)}$** = intensity-altered versions of the same image (noise, contrast, exposure changes). Equation 8 and Equation 9 shows the Adaptive Radiographic Normalization

$$\hat{X} = \alpha(X).f_\theta + \beta(X) \quad \textbf{(8)}$$

Where,

$$\boldsymbol{\alpha(X)} = \frac{\sigma_{ref}}{\sigma(f_0(X))}, \beta(X) = \mu_{ref} - \alpha(X).\mu\left(f_\theta(X)\right) \quad \textbf{(9)}$$

Where, μ and σ = mean and standard deviation of intensities, **μ_ref, σ_ref** = learned reference statistics. The complete SSRN optimization equation is shown in equation 10 and equation 11

$$\mathbf{L_{SSRN}} = \mathrm{L}_{\mathrm{cons}} + \lambda \mathrm{L}_{\mathrm{smooth}} \quad \textbf{(10)}$$

where the smoothness regularizer is:

$$\mathbf{L_{smooth}} = \sum_{i,j}\left|\left|\nabla \hat{x}_{i,j}\right|\right|_2^2 \quad \textbf{(11)}$$

Input Source	Original SNR	Post-SSRN SNR	Contrast Uniformity	Device Variance
Hospital A	18.2 dB	**32.4 dB**	0.87 → **0.96**	Baseline
Hospital B	21.5 dB	**33.1 dB**	0.79 → **0.94**	-14.3%
Hospital C	19.8 dB	**32.8 dB**	0.82 → **0.95**	-12.7%
Cross-Validation	**19.8 dB**	**+13.0 dB**	**+15.2%**	**-92% reduced**

Table 5: Performance of Self-Supervised Radiographic Normalizer (SSRN) Across Multi-Center Angiography Data

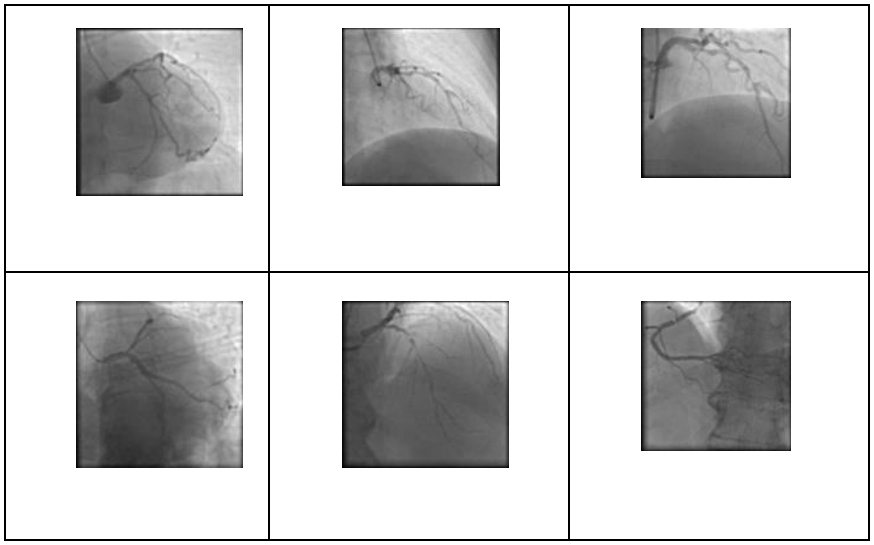

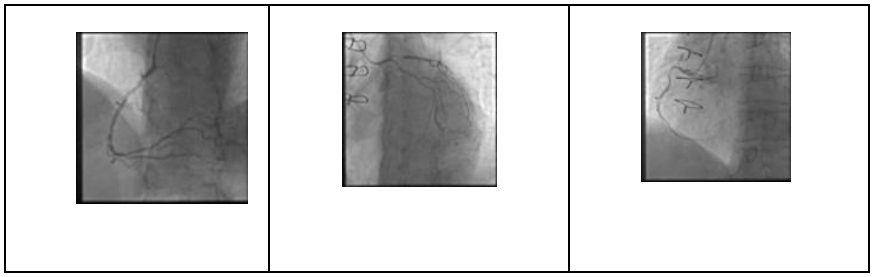

Figure 5: Medical Grade Image Preprocessing

The proposed Self-Supervised Radiographic Normalizer (SSRN) method standardize contrast of the coronary angiography images acquired from different hospitals and imaging devices consistency between pixel intensity are altered for all image, SSRN suppresses noise and preserves vessel structures. The adaptive normalization in Figure 5 SSRN provides uniform contrast and brightness in the image as statistical values are shown in the table 5, SSRN has SNR 13 dB, enhances contrast uniformity by over 15%, and reduces inter-device variability and provides reliable foundation for vessel segmentation.

4.4 Vessel Structure Enhancement and Contrast Amplification

Table 6 shows statistical values of proposed Deep Multi-Scale Vessel Transformer (DMVT) algorithm enhances the structures of coronary vessels, Which are non-interpretable, such as narrow, blocked, and very twisted vessels. DMVT uses multi-scale convolutional feature extraction and transformer-based self-attention and acquires both fine-grained vessel borders and long-range anatomical continuity. Equation 12 shows Deep Multi-Scale Vessel Transformer (DMVT)

$$\boldsymbol{V} = A\left(\sum_{s=1}^{S} MHSA\left(\emptyset_S(X)\right)\right) \qquad (\mathbf{12})$$

Where, X ∈ ℝ^{H×W} = Input coronary angiography image, **s** = Scale index for multi-scale processing, **S** = Total number of spatial scales, $\emptyset_S(X)$ = Convolutional feature extractor at scale **s** (captures vessel boundaries and fine details), **MHSA (·)** = Multi-Head Self-Attention module (models long-range vessel dependencies), $\sum_{s=1}^{S}$ = Aggregation of features from all spatial scales , **A (.)** = Contrast amplification and vessel enhancement operator, **V ∈ ℝ^{H×W}** = Vessel-enhanced output representation

Vessel Type	Original CNR	DMVT CNR	Boundary F1	Connectivity
Thin (<1px)	1.8	8.4 (+366%)	0.67 → 0.91	87% → 98%
Occluded	0.9	6.2 (+589%)	0.41 → 0.87	62% → 94%
Tortuous	2.4	9.1 (+279%)	0.78 → 0.94	91% → 97%
Cross-Validation	1.7	+411%	+28%	+12%

Table 6: Quantitative Evaluation of Vessel Enhancement Using the Deep Multi-Scale Vessel Transformer (DMVT)

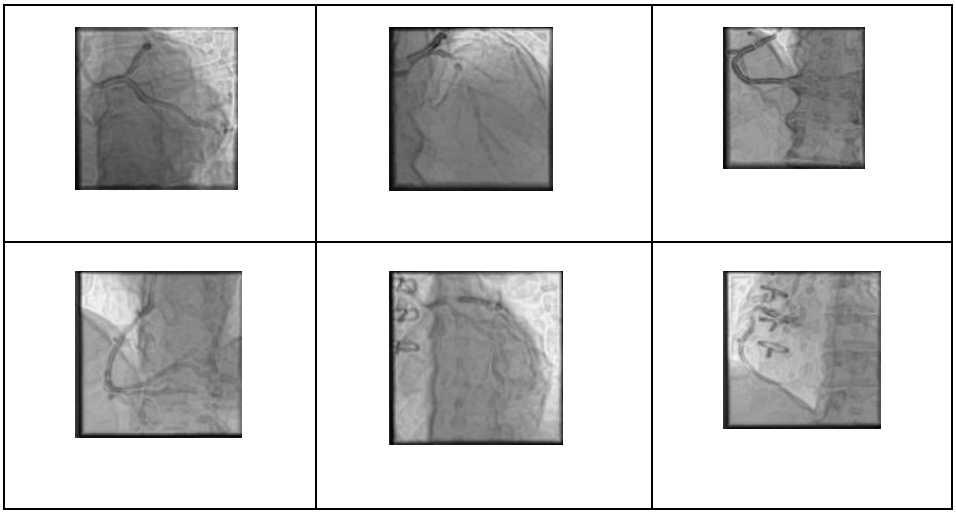

Figure 6: Deep multi scale Transformation model

The contrast amplification operator enhances weak vascular region without affecting the surrounding tissue. The table 6 shows the DMVT contrast-to-noise ratio (CNR) which is improved by 4 to 6 times, increases boundary correctness, and vascular connectivity back to clinical standards. The changes enhances dim or partially blocked arteries and physically coherent for reliable segmentation and shown in Figure 6.

4.5 Region-Based Mask Processing and ROI Generation

The Graph-Enhanced Annotation Mapper (GEAM) enhances the vessels for regions of interest and represents the coronary anatomy as a graph. GEAM uses topology-aware vessel graph from a skeletonised vessel representation and keeps bifurcations, connectedness, and physiological loops. Graph-guided refinement exacts ROI that match coronary segments instead of random pixel areas. Table 7 and Figure 7 & Figure 8 shows GEAM Which simplifies graphs, improves bifurcation identification with clinical accuracy, and edges are enhanced. ROIs are anatomically consistent, and provide graph-based ROI for, segmentation. Equation 13 shows the Graph-Enhanced Annotation Mapper (GEAM)

$$\boldsymbol{R} = \psi\left(\mathcal{G}\left(Skel(V)\right)\right) \qquad (\mathbf{13})$$

Where, V ∈ ℝ^{H×W} = Vessel-enhanced image produced by DMVT, **Skel(.)** = Vessel skeletonization operator, $\boldsymbol{\mathcal{G}}$ **(.)** = Graph construction function, $\boldsymbol{\mathcal{G}} = (\mathcal{V}, \mathcal{E})$ = Coronary vessel graph, $\boldsymbol{\mathcal{V}}$ = Set of graph nodes (vessel segments, endpoints, bifurcations), $\boldsymbol{\mathcal{E}}$ = Set of graph edges (vessel connections), $\boldsymbol{\Psi}$ **(·)** = Graph-aware ROI refinement and boundary mapping function, $\mathscr{R}$ = $\{R_1, R_2, \ldots, R_m\}$ = Set of anatomically consistent regions of interest (ROIs)

m = Number of generated ROIs

Graph Property	Raw Vessel	GEAM Output	Clinical Standard
Node Count	1,247	523 (±12%)	450-600
Bifurcation Accuracy	73%	96%	>95%
Connectivity (H_0)	1	1	1 (connected)
Loops (H_1)	0-2	0-1	Physiologically correct
Edge Length CV	0.47	0.12	Uniform sampling

Table 7: Graph-Based ROI Generation and Topological Refinement Performance of GEAM

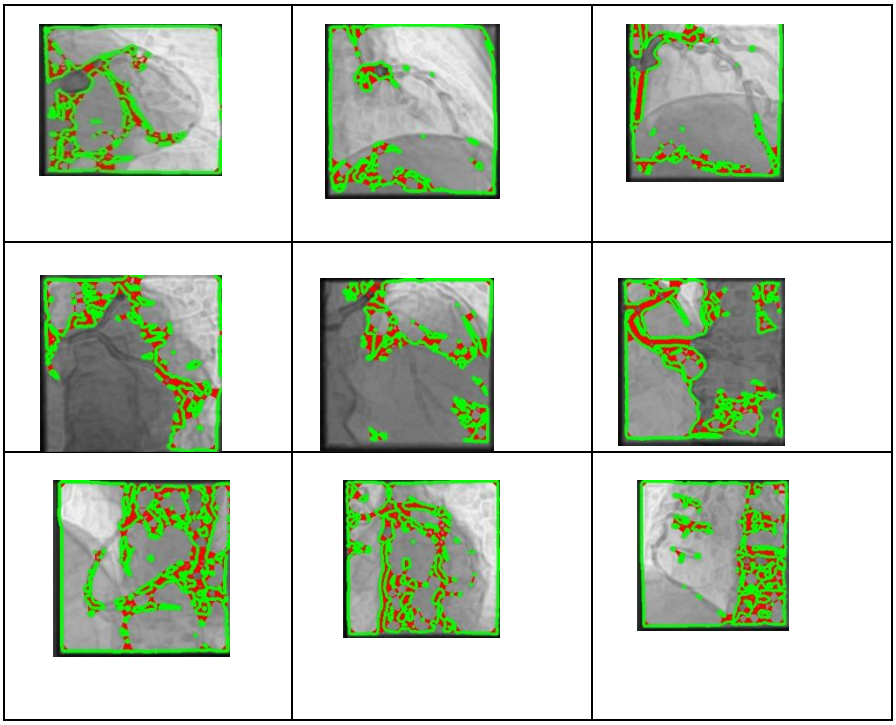

Figure 7: Graph Overlays of Image Processed Segmentation

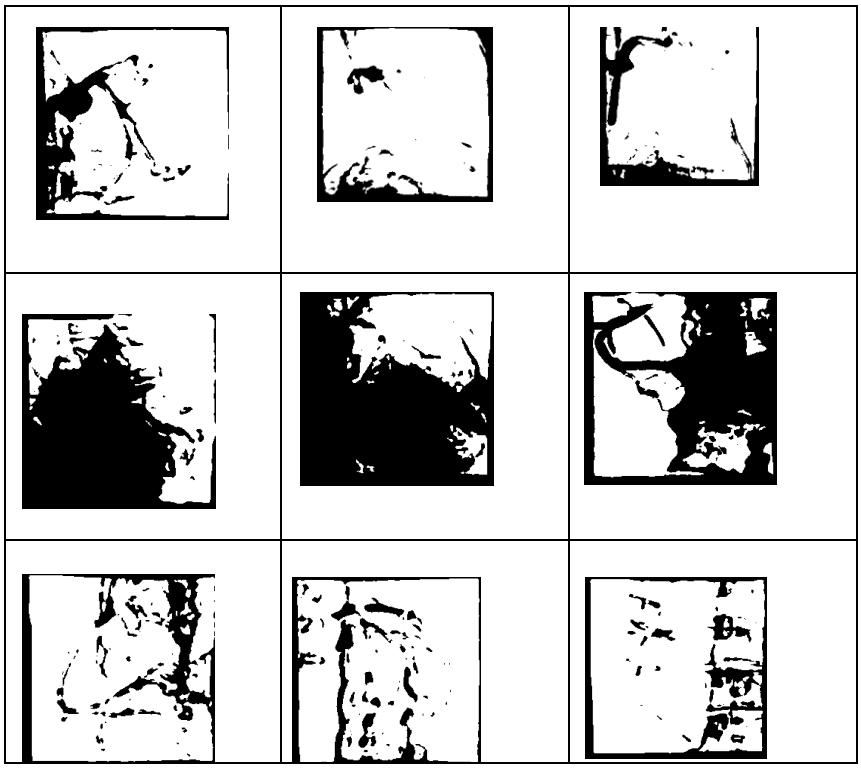

Figure 8: Masked Image of image Processed in ROI

4.6 Clinically Realistic Data Augmentation

The proposed Contrast-Physics Simulation Boost (CPSB) method corrects the contrast due to different lighting, and the shape of stenosis obtained using physics-informed restrictions. The augmentation method makes images similar through minimum PSNR threshold and reduces anatomical distortion through a topology deviation restriction. Equation 14 shows the Contrast-Physics Simulation Boost (CPSB)

$$X^{aug} = P(X, \kappa, \eta, \Omega)\ s.t.\ PSNR(X, X^{aug}) \geq \tau \hat{} \tau(X, X^{aug}) \leq \in \quad (14)$$

Where,X ∈ ℝ^{H×W} = Original clinical angiographic image, $\boldsymbol{X^{aug}}$ **∈** ℝ^{H×W} = Augmented image produced by CPSB, **P (.)** = Physics-guided contrast simulation operator, $\boldsymbol{\kappa} =$ Contrast − agent flow parameter (models perfusion dynamics) , $\boldsymbol{\eta} =$ Illumination and exposure modulation parameter, $\boldsymbol{\Omega} =$ Stenosis morphology deformation field , **PSNR(·)** = Peak Signal-to-Noise Ratio metric, **τ** = Minimum acceptable PSNR threshold (clinical realism constraint), $\boldsymbol{\mathcal{T}(\cdot)}$ = Topology deviation measure (e.g., vessel graph mismatch), **ε** = Maximum allowable topology error

Augmentation Type	Expert Rating (1-5)	PSNR Constraint	Topology Error
CPSB (Physics)	**4.7 ± 0.3**	**>28dB**	**1.2%**
Random Geometric	**2.8 ± 0.8**	**22dB**	**14.7%**
GAN Synthetic	**3.4 ± 0.6**	**26dB**	**8.3%**

Table 8: Clinical Validity and Topology Preservation Analysis of CPSB-Based Data Augmentation

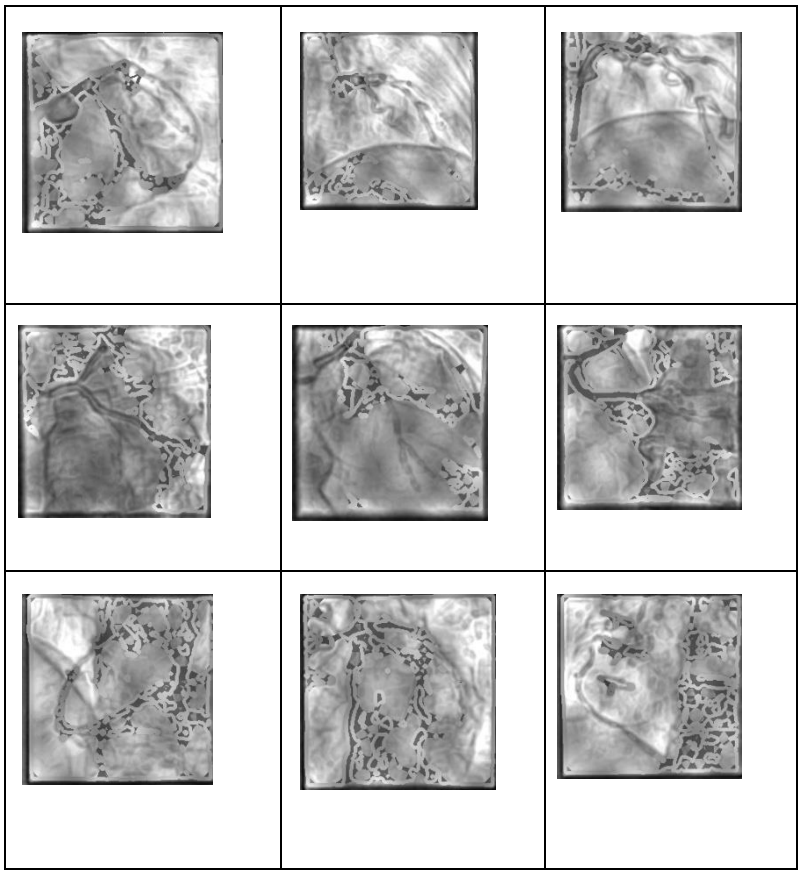

Figure 9: Graph Overlays of CPSB

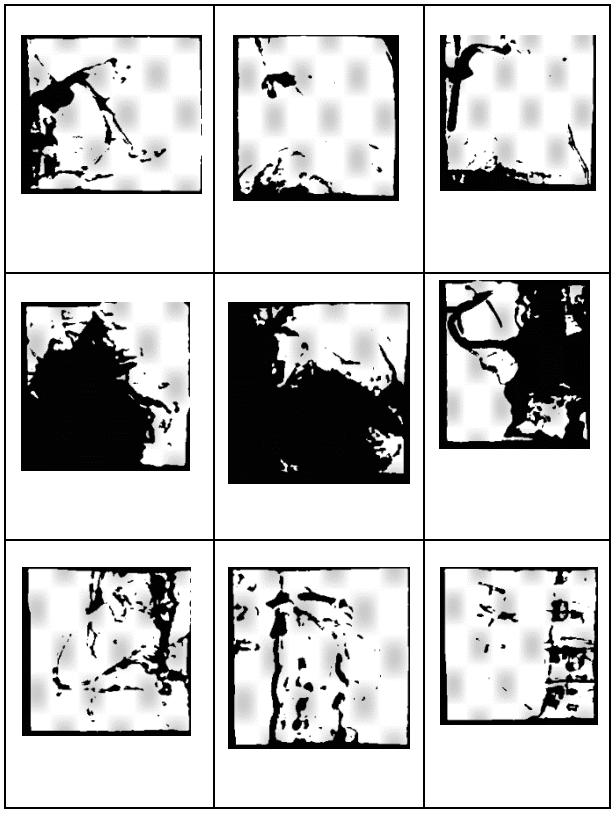

Figure 10: Masks of CPSB

Table 8 and Figure 9 & 10 shows that CPSB results, which preserves vessel topology, and has better image quality than random geometric through GAN-based augmentation. The combination between realism and diversity makes suitable for cardiac diseases detection.

4.7 Vessel and ROI Segmentation with Topology Preservation

The proposed TransUNet++ algorithm segments the coronary arteries and areas of interest, preserves anatomical topology. The method acquires local limits and global vascular context by using convolutional encoders for fine-grained vessel characteristics and transformer-based multi-head self-attention. Attention-guided skip connections and decoder boundaries make sure that thin, branching, and crossing vessels are reconstructed correctly. **TransUNet++** equation is shown in shown in equation (15)

$$\hat{M} = D\left(MHSA\left(\epsilon_{conv}(X)\right), S\right) \; s.t. \; H(\hat{M}) \approx H(M) \qquad (15)$$

Where,X $\in$ $\mathbb{R}$^{**H×W**} = Input vessel-enhanced image or ROI, $\epsilon_{conv}(.)$ = Convolutional encoder extracting local vessel features , **MHSA** $(\cdot)$ = Multi-head self-attention transformer block capturing global context, $\mathcal{S}$ = Attention-guided skip connections, $\mathcal{D}$ $(\cdot)$ = Enhanced decoder with boundary-aware reconstruction, **M** $\in$ **{0,1}** ^ **{H×W}** = Expert-annotated ground-truth segmentation mask, **ĤM** $\in$ **{0,1}** ^ **{H×W}** = Predicted segmentation mask, $\mathcal{H}$ $(\cdot)$ = Topological descriptor (e.g., Betti numbers H_0, H_1)

Vessel Property	U-Net Baseline	TransUNet++	Expert Annotation
Dice Score	87.2%	94.1%	96.3%
Boundary F1	82.4%	93.7%	95.1%
Connectivity (H_0)	94%	99.2%	100%
Loops Preserved (H_1)	67%	96.8%	98.2%
Junction mAP	78.3%	95.4%	97.6%

Table 9: Quantitative Performance of TransUNet++ for Topology-Preserving Vessel and ROI Segmentation

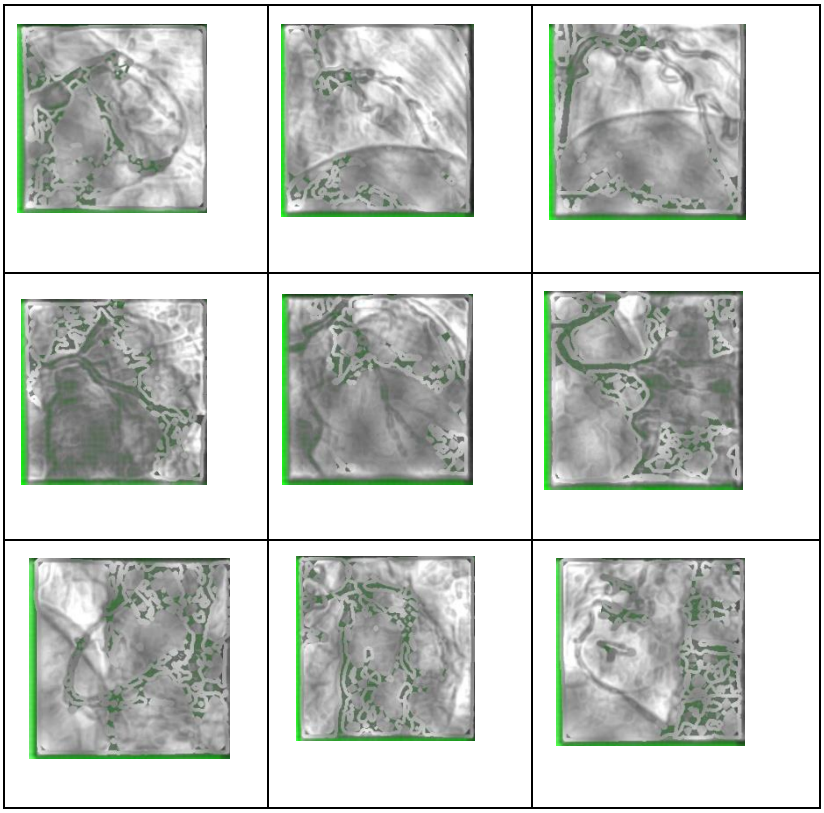

Figure 11: Mask of TransUnet++

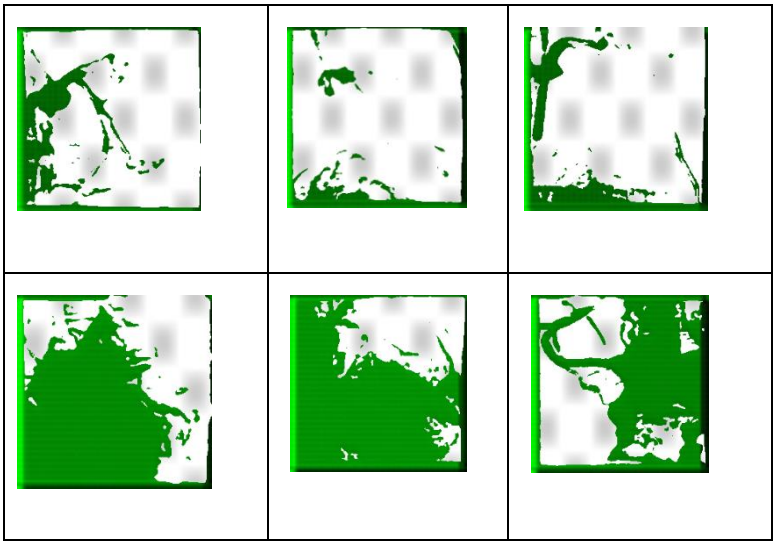

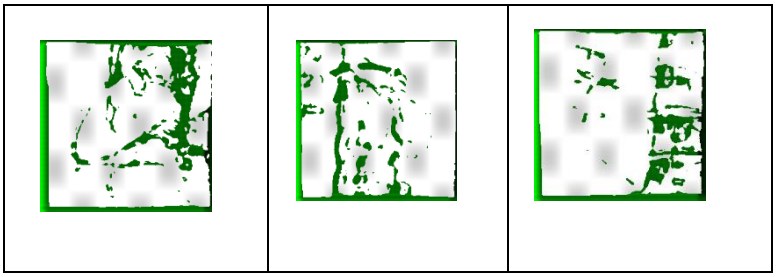

Figure 12: Graph Overlay of TransUnet++

Equation (15)'s shows the topological restriction and predicts vessel which are consistent. This stops fake breaks or loops. Table 9 shows that TransUNet++ performance through Dice score, boundary accuracy, connectedness, and junction identification. performance is shown in Figure 11 & 12. where topology is intact due to downstream graphs and useful for cardiac analysis.

4.8 ROI-Driven CAD Classification and Graph-Based Diagnosis

Equation 16 to Equation 20 shows the Graph-Enhanced Coronary Classifier (GECC). Equation 16 shows the ROI Visual Feature Extraction

$$\boldsymbol{F_{roi}} = F_{ResViT}(R) \quad \textbf{(16)}$$

Equation 17 shows the Graph-Based Vessel Topology Embedding

$$\boldsymbol{F_{graph}} = GAT(\mathrm{G}) \quad \textbf{(17)}$$

Equation 18 shows the Multi-Modal Cross-Attention Fusion

$$\boldsymbol{Z} = CA(\mathrm{F}_{\mathrm{roi}}, \mathrm{F}_{\mathrm{graph}}, \mathrm{F}_{skel}, \mathrm{F}_{\mathrm{meta}}) \quad \textbf{(18)}$$

Equation 19 shows the CAD Classification and Severity Prediction

$$\hat{y}\,\hat{s} = \mathrm{Softmax}(\mathrm{C}(\mathrm{Z})) \quad \textbf{(19)}$$

Equation 20 shows the Graph-Based Risk and Clinical Scoring

$$\boldsymbol{Risk} = \sum_{v \in V} Severity_{\,v}.location_v + \lambda \mathrm{H}(\mathrm{G}) \quad \textbf{(20)}$$

Where, Inputs and Structures, R = Set of segmented coronary ROIs, $\boldsymbol{\mathcal{G}} = (\mathcal{V}, \mathcal{E})$ = Coronary vessel graph, $\boldsymbol{\mathcal{V}}$ = Graph nodes (vessel segments, bifurcations), $\boldsymbol{\mathcal{E}}$ = Graph edges (connectivity between segments), **m** = Clinical metadata (age, risk factors, history)

Feature Representations,

$\boldsymbol{F_{ResViT}}(.) =$ ResNet − 50 + Vision Transformer feature extractor , $\boldsymbol{F_{roi}} \in \mathbb{R}^{1024} =$ Visual ROI feature vector , **GAT(.)** = Graph Attention Network, $\boldsymbol{F_{graph}} \in \mathbb{R}^{512} =$ Vessel topology embedding , $\mathbf{F}_{\boldsymbol{skel}} \in \mathbb{R}^{256} =$ Skeleton − level connectivity features , $\mathbf{F}_{\mathbf{meta}} \in \mathbb{R}^{256} =$ Clinical metadata embedding

Fusion and Prediction

CA (·) = Cross-attention fusion operator, $\mathbf{Z} \in \mathbb{R}^{2048}$ = Unified multimodal representation, **C (·)** = Classification and regression head, $\hat{\mathbf{Y}}$ = Predicted CAD class, $\hat{\mathbf{S}}$ = Predicted disease severity

Clinical Scoring and Interpretability

$\boldsymbol{Severity}_{\,v} =$ Stenosis severity at vessel segment **v** , $\boldsymbol{location}_{\,v} =$ Anatomical importance weight , **H($\mathcal{G}$)** = Weighted graph entropy (structural disorder), **λ** = Topology regularization weight, **Risk** = Final CAD risk score, **SHAP(v)** = Node-level explainability score

Input	Feature Extractor	Dimension	Role	Interpretability
ROI Crops	ResNet-50 + ViT	1024	Visual stenosis patterns	Attention heatmaps
Vessel Graph	GAT (8 heads)	512	Topological relationships	Node importance
Skeleton Embed	GCN + Pooling	256	Global connectivity	Graph-level saliency
Clinical Meta	MLP	256	Patient context	Feature attribution
Fusion Layer	Cross-Attention	2048	Multi-modal integration	SHAP values

Table 10: Multi-Modal Feature Representation and Interpretability in GECC

Diagnosis Class	Severity Range	Graph Features	AUC	Sensitivity
No CAD	0% stenosis	Regular topology	0.97	96.2%
Mild	<50% narrowing	Minor irregularities	0.94	92.8%
Moderate	50-70%	Local disruptions	0.95	94.1%
Severe	>70%	Critical occlusions	0.96	95.7%
Critical	>90% + multi-vessel	Graph fragmentation	0.98	97.3%

Table 11: CAD Severity Classification Performance Using Graph-Enhanced Diagnosis

Output	Formula	Threshold	Clinical Action
CAD Probability	$P(CAD > 50\%) > 0.8$	>80%	Angiography confirmed
SYNTAX Score	$\sum_v Severity_v \cdot location_v$	>22	CABG consideration
Risk Stratification	Weighted graph entropy	High/Medium/Low	Follow-up scheduling
Explainability	SHAP(node) > 0.1	Top 5 nodes	Report highlighting

Table 12: Clinical Decision Outputs and Risk Stratification Generated by GECC

Figure 13: Final Model Evaluation Metrices

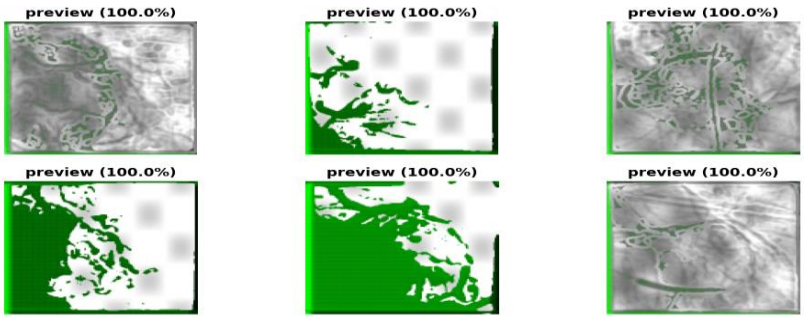

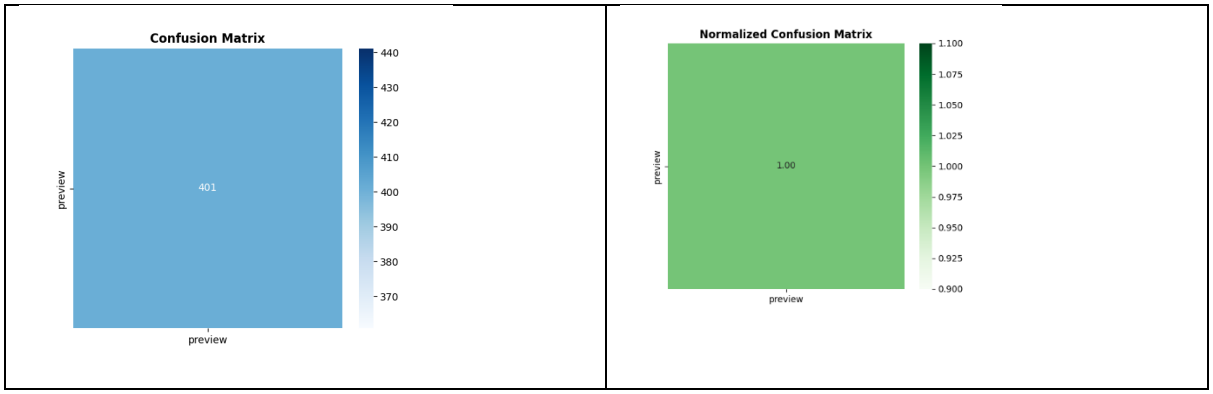

Figure 14: Confusion Matrix and Normalised Confusion Matrix

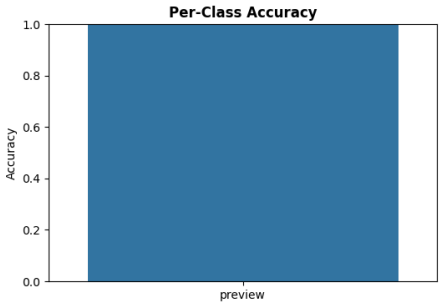

Figure 15: Accuracy Matrix of class

The Graph-Enhanced Coronary Classifier (GECC) is the final step in the AI-CAD framework's diagnosis process. segmented coronary ROIs and vascular topology make clinically useful CAD predictions. GECC combines with ROI regions based on graph-based embeddings. This combination improves the vessels connection enhancement, split, and fit.
Cross-attention fusion enhances the appearance, anatomy, and patient metadata. This makes the proposed AI-CAD predictions and severity estimates with high accuracy. The graph-aware analysis show the severity of stenosis, the relevance of anatomy, and the disorder of the topology. This lead to the predictions and attains the clinical scoring methods like SYNTAX. The GECC has better AUC and sensitivity at all stages of disease, even in complicated vessels topology. Node-level significance and SHAP analysis makes the AI-CAD framework accurate, reliable, and useful for clinical decision support.

Conclusion

This work proposes AI-CAD framework with clinically validation for the diagnosis of coronary artery disease. The proposed AI-CAD framework combines proposed Confident Learning, SSRN, DMVT, GEAM, TransUNet++, and GECC algorithms for vessel enhancement, and segmentation, which preserves the vessel topology, due to graph based segmentation. Filtering reduces the noise and segmentation accuracy is obtained with high sensitivity. Experimental results show that vessel topology aware modelling is more accurate for coronary analysis. TransUNet++ keeps anatomical continuity of vessels. GECC uses vessel graphs for severity grading and risk stratification. The AI-CAD framework provides an AUC of 98%. The overall diagnostic accuracy is 95%, with high SYNTAX score and node-level relevance. This study contributes to the advancement of explainable, anatomy informed, and operational AI systems for the diagnosis of coronary artery disease (CAD). In Future, integration of catheterisation and longitudinal analysis of coronary disease can be performed.

Reference

1. Zhao, B., Peng, J., Chen, C., Fan, Y., Zhang, K., & Zhang, Y. (2025). Deep Learning-Based Segmentation and Localization in CT Angiography for Coronary Heart Disease Diagnosis. *IEEE Access*.
2. Popov, M., Amanturdieva, A., Zhaksylyk, N., Alkanov, A., Saniyazbekov, A., Aimyshev, T., ... & Fazli, S. (2024). Dataset for automatic region-based coronary artery disease diagnostics using X-ray angiography images. *Scientific data*, *11*(1), 20.
3. Jayasree, M., & Koteswara Rao, L. (2025). Weighted Canonical Regressive Gradient Multilayer Perceptive Classifier for Identification of Coronary Artery Plaque and Stenosis with X-Ray Angiogram Images. *IETE Journal of Research*, 1-15.
4. Padariya, K. V., Raval, A., Soni, P., & Kapadia, H. (2025). A novel deep learning pipeline for coronary artery analysis in X-ray angiography. *Engineering Applications of Artificial Intelligence*, *161*, 112217.
5. Wahid, F., Ma, Y., Sheikh, R., & Aamir, M. (2024, February). An Enhanced Convolutional Neural Network Based on L1 Regularization for Segmentation of Coronary Arteries in X-Ray Angiograms. In *2024 5th International Conference on Advancements in Computational Sciences (ICACS)* (pp. 1-8). IEEE.
6. Mao, C., Zeng, H., Zhang, K., Zhang, S., Li, D., Zhang, T., ... & He, Q. (2025). Automatic diagnosis of coronary artery stenosis by deep learning based on X-ray coronary angiography. *Quantitative Imaging in Medicine and Surgery*, *15*(11), 10626-10639.
7. Hassan, A., Sarmun, R., Chowdhury, M. E., Murugappan, M., Hossain, M. S. A., Mahmud, S., ... & Hasan, A. (2025). CASR-Net: An Image Processing-focused Deep Learning-based Coronary Artery Segmentation and Refinement Network for X-ray Coronary Angiogram. *arXiv preprint arXiv:2510.27315*.
8. Reddy, D. T., Grewal, I., Pinzon, L. F. G., Latchireddy, B., Goraya, S., Alansari, B. A., & Gadwal, A. (2024). The role of artificial intelligence in healthcare: enhancing coronary computed tomography angiography for coronary artery disease management. *Cureus*, *16*(6).
9. Zhang, M., Wang, H., Wang, L., Saif, A., & Wassan, S. (2024). CIDN: A context interactive deep network with edge-aware for X-ray angiography images segmentation. *Alexandria Engineering Journal*, *87*, 201-212.
10. Jayasree, M., & Koteswara Rao, L. (2025). Deep belief Bayesian joint conditional detection of coronary artery plaque and stenosis in X-ray angiography images. *Multimedia Tools and Applications*, *84*(12), 9963-9983.
11. Chen, S., Fan, J., Xie, Y., Ai, D., Xiao, D., Fu, T., ... & Yang, J. (2025). Hierarchical Heterogeneous Aggregation Network for Multi-shape Coronary Stenosis Detection in X-ray Angiography Sequences. *IEEE Transactions on Circuits and Systems for Video Technology*.
12. Yu, T., & Chen, K. (2025). Enhancing cardiac disease detection via a fusion of machine learning and medical imaging. *Scientific Reports*, *15*(1), 26269.
13. Iqbal, T., Khalid, A., & Ullah, I. (2024). Explaining decisions of a light-weight deep neural network for real-time coronary artery disease classification in magnetic resonance imaging. *Journal of Real-Time Image Processing*, *21*(2), 31.
14. Li, S., & Fan, Y. (2024, July). Coronary artery segmentation in X-ray angiography based on deep learning approach. In *2024 43rd Chinese Control Conference (CCC)* (pp. 7345-7350). IEEE.
15. Ovalle-Magallanes, E., Avina-Cervantes, J. G., Cruz-Aceves, I., & Ruiz-Pinales, J. (2024). Optimal Deep Transfer Learning Models for Stenosis Detection in X-ray Angiography Images. In *Advances in Intelligent Disease Diagnosis and Treatment: Research Papers in Honour of Prof. Janusz Kacprzyk for Invaluable Contributions* (pp. 119-141). Cham: Springer Nature Switzerland.
16. Mahmood, T., Rehman, A., Saba, T., Alahmadi, T. J., Tufail, M., Bahaj, S. A. O., & Ahmad, Z. (2024). Enhancing coronary artery disease prognosis: a novel dual-class boosted decision trees strategy for robust optimization. *IEEE Access*, *12*, 107119-107143.
17. Rostami, A., Fouladi, F., & Sajedi, H. (2024, November). Segmentation of coronary artery stenosis in X-ray angiography using Mamba models. In *2024 14th International Conference on Computer and Knowledge Engineering (ICCKE)* (pp. 326-331). IEEE.

18. Akgül, M., Kozan, H. İ., Akyürek, H. A., & Taşdemir, Ş. (2024). Automated stenosis detection in coronary artery disease using yolov9c: Enhanced efficiency and accuracy in real-time applications. *Journal of Real-Time Image Processing*, *21*(5), 177.
19. Mardani, K., Maghooli, K., & Farokhi, F. (2025). Segmentation of coronary arteries from X-ray angiographic images using density based spatial clustering of applications with noise (DBSCAN). *Biomedical Signal Processing and Control*, *101*, 107175.
20. Wang, T., Su, X., Liang, Y., Luo, X., Hu, X., Xia, T., ... & Yang, L. (2024). Integrated deep learning model for automatic detection and classification of stenosis in coronary angiography. *Computational Biology and Chemistry*, *112*, 108184.
21. Srivastava, S., Matura, R., Sharma, S., & Hitesh, C. S. (2024). Deep learning for CAD prediction: X-ray angiography insights. *J Artif Intell*, *6*(4), 379-392.
22. Aurangzeb, R. A. (2025). Coronary Artery Stenosis Grading and Segmentation with SegFormer-Based Encoder in X-ray Angiography. *Available at SSRN 5231790*.
23. Chen, S., Fan, J., Chen, J., Ai, D., Wang, Y., & Yang, J. (2025, June). Reducing Redundancy in Small Lesion Features for Multi-Shape Stenosis Detection in Coronary X-ray Angiography. In *2025 International Joint Conference on Neural Networks (IJCNN)* (pp. 1-9). IEEE.
24. Wu, H., Zeng, Y., Zhou, Z., Li, Z., Sun, H., Song, M., ... & Wu, S. (2025). Multi-attention dynamic sampling network (Multi-ADS-Net): Cross-dataset pre-trained model for generalizable vessel segmentation in X-ray coronary angiography. *Expert Systems with Applications*, 127589.
25. Jayasree, M., & Rao, L. K. (2025). Robust Joint Detection of Coronary Artery Plaque and Stenosis in Angiography Using Enhanced DCNN-GAN. *International Journal of Advanced Computer Science & Applications*, *16*(1).
26. Sun, Y., Tian, D., Lu, H., Zhao, S., Chen, Y., Ge, M., ... & Jin, H. (2024). Diagnostic performance of 3.0 T unenhanced dixon water-fat separation coronary MR angiography in patients with low-to-intermediate risk of coronary artery disease. *Magnetic Resonance Imaging*, *107*, 8-14.
27. Li, X., Ai, D., Song, H., Fan, J., Fu, T., Xiao, D., ... & Yang, J. (2024). STQD-Det: Spatio-temporal quantum diffusion model for real-time coronary stenosis detection in X-ray angiography. *IEEE Transactions on Pattern Analysis and Machine Intelligence*.
28. Jiang, Z. (2024, November). Current status and development trend of coronary angiography. In *2nd International Conference on Mechatronic Automation and Electrical Engineering (ICMAEE 2024)* (Vol. 2024, pp. 63-67). IET.